Ultra Wideband Wireless Propagation Channel Characterizations for Biomedical Implants

Bao-Lin Wei, Chun Xiong, Hong-Wei Yue, Xue-Ming Wei, Wei-Lin Xu, Qian Zhou, and Ji-Hai Duan

Abstract—In order to inspect the feasibility and safety of wireless communication operated in 3.1-5.0 GHz band between the devices located in vivo and on body or off-body, the path gain and specific absorption rate (SAR) were investigated through embedding a high-resolution 3D electromagnetic model of human body into a numerical electromagnetic (EM) simulator which is based on finite integration technique (FIT) to solve the Maxwell equations. Based on the electromagnetic (EM) simulating results, a channel numerical statistical model depicting the in vivo distance-depended channel path gain was proposed. The experimental results indicate that it is feasible and safe for the wireless communication of implantable devices in 3.0-10.5 GHz band. The in vivo distance-depended path gain can be modeled by a modified classical power law function, and the averaged root-mean-square error (RMSE) between the computational results of numerical statistical model and EM simulation is 9.8.

Index Terms — electromagnetic model of human body, electromagnetic radioactive, ultra wideband (UWB), finite integration technique (FIT), implantable devices

I. INTRODUCTION

WITH the development of medical technology, more and more sophisticated biomedical devices are used for diverse applications, such as telemedicine systems, remote health monitoring, body implantable devices, and so on[1-3]. The physiological data of patients can be measured with the aid of electronic devices located on or inside the human body and transmitted wirelessly to an external receiver for processing, thereby enhancing the health monitoring, diagnosis, and therapy of the patients. In-body medical implantable devices are typically battery-operated, and once implanted, they should operate for several years and consume as little power as possible. Furthermore, more and more advanced implantable devices need high data rate, low complexity, and small size. For instance, a multi-channel neural recording system needs more than 100 Mbps data rate [4], and a capsule endoscope needs more than 10 Mbps data rate [5]. The Medical Implant Communication System (MICS) which is in the band of 402-405 MHz, has been applied to implantable medical devices by the US Federal Communications Commission (FCC), and it has suitable propagation characteristics of going through human tissues. However, MICS only provides a maximum data rate of 800 Kbps, and it belongs to narrow-band standard and needs power hungry components like voltage controlled oscillator (VCO), phase locked loop (PLL) and analog to digital converter (ADC). Due to the inherent characteristics of simple electronics and high transmission speed, ultra wideband (UWB) technology has great potential to satisfy the needs of the next generation implantable devices' aforementioned characteristics, and becomes a promising candidate [5]. In particular, impulse radio UWB (IR-UWB), the simplest form of UWB, is a promising low complexity solution. An IR-UWB transmitter which is always implanted in the body is simple to design and has lower power consumption. Contrarily, complexity is more on the receiver side which is always located on the body or off the body. Moreover, the power consumption of IR-UWB scales down with data rates.

The designs and architectures of communication system are influenced by the transmission rates, the wave propagation channel, modulation and demodulation schemes, and the system power consumption [5]. To provide a clear understanding of the communication link between the implanted device and the transceiver located outside the human body, it is essential to analyze the wave attenuation in high-loss human tissues and propagation in the vicinity of the human body. Moreover, accurate knowledge of the propagation channel and strategies to optimize the communication link quality is necessary for efficient design of implantable UWB wireless communication systems. However, currently, there is no standard model of the UWB channel properties for in-body medical implants due to the unavailability of measurements and the complexity of simulations for the frequency-dependent tissue properties of the human tissues or organs [5].

Considerable research efforts have been devoted to characterizing the propagation characterization of radio waves for on-body or in-body devices [2, 6-8]. The characterization of the UWB communication link of chest-to-waist and chest inside-to-outside was presented in [6], but the frequency band only covered the lower band of UWB from 3.4 GHz to 4.8 GHz. The wave propagation for line-of-sight (LOS) scenarios in the frequency bands of 100-1000 MHz and 1-5 GHz were evaluated in [2] by using a model of the human torso and, a second-order polynomial was used to approximate the permittivity of human tissues calculated from the Gabriel's four-pole Cole-Cole equation, which simplified the calculation. However, the permittivities of human tissues are frequency-dependent complicated

variables and the same tissue has different permittivity in different frequency. Therefore, it was cursory to evaluate the average power density in a wide frequency band over 1-5 GHz in [2]. In [7], several different human tissues' electrical parameters were used to define each layer as a specific dielectric material in a multi-layer model which was implemented in HFSS (High Frequency Structure Simulator) to investigate the channel path loss of implantable wireless link. However, the multi-layer model was too simple to well characterize the complicated real human body. The in-body propagation characterization presented in [8] only covered 2.5 GHz and 3.5 GHz.

To more accurately characterize the propagation channel between in-body implanted devices and on-body or off-body devices in the frequency band of 3.0-10.5 GHz, this paper performed electromagnetic simulation based on a high resolution electromagnetic model of human body which was comprised of 85 kinds of tissues or organs and constructed from living human body's computed tomography (CT) and magnetic resonance imaging (MRI) images. The average power density of electromagnetic field in the body and the specific absorption rate (SAR) absorbed by the human body were also explored to investigate the validity of implantable communication in this band. Finally, the distance-dependent path gain for inside body was modeled based on the average power density.

II. ELECTROMAGNETIC HUMAN BODY MODEL AND SIMULATION SCENARIO

A. Electromagnetic Model of Human Body

Different from typical wireless communications through the free space, the main difficulty for in-body UWB channel propagation modeling is the frequency-dependent material properties of different human tissues and organs which must be considered in the calculations. The various tissues and organs within the human body have their own unique conductivity, dielectric constant, thickness, and complex geometry. On the other hand, the electromagnetic properties of different human tissues, such as the permittivity and conductivity, depend largely on the frequency and therefore can only be considered constant over a narrow range of frequencies. The complex relative permittivities as a function of angular frequency for human body tissues have been made available based on the four-pole Cole-Cole equations, by Gabriel [9]:

$$\hat{\varepsilon}(\omega) = \varepsilon_\infty + \sum_n \frac{\Delta\varepsilon_n}{1+(j\omega\tau_n)^{(1-\alpha_n)}} + \frac{\sigma_i}{j\omega\varepsilon_0}. \qquad (1)$$

This equation was derived from the well-known Debye expression, in which ε_∞ is the permittivity at field frequencies with $\omega\tau \Box 1$, ω is angular frequency, σ_i is the static ionic conductivity and ε_0 is the permittivity of free space, the distribution parameter, α_n, is a measure of the broadening of the dispersion, and τ_n is the relaxation time for each dispersion region. For a known relative permittivity, the conductivity can be obtained by equation:

$$\sigma = \frac{\alpha}{\pi f}\sqrt{\frac{\alpha^2}{\mu_0^2}+\frac{\omega^2\varepsilon_0\varepsilon_r}{\mu_0}}. \qquad (2)$$

In this equation, α is attenuation coefficient, ε_r is relative permittivity, μ_0 is magnetic permeability of free space, and f is frequency. It is shown from (1) and (2) that the permittivity and conductivity are complex functions of angular frequency respectively. Therefore, they can only be considered constant over a narrow range of frequencies.

In order to investigate the characteristics of UWB wireless communication link in/through the human body, the body has to be characterized as a medium for wave propagation, and a high resolution electro-magnetic model of human body would be constructed. The accuracy of EM calculation is determined by the resolution of the electromagnetic human vowel model. This paper has constructed an electromagnetic model of human body based on CT and MRI slices data provided by Yale University [10]. The model was constructed from 498 slices, and the slices images of torso and head were taken from a living human male, the slices of arms and legs were from the Visible Human Project (VHP) of National Library of Medicine [11] by Stuchly. A sample of the cut view image is illustrated in Fig. 1(a). The original images were reconstructed in a 512×512 matrix with a resolution of 1 mm in the x, y planes; the z-axis resolution is 1 cm from neck to mid-thigh and 0.5 cm from neck to crown of the head. The proposed 3D electromagnetic model of human body is shown in Fig. 1(b). It is with 3.6×3.6×3.6 mm³ resolution.

The more human tissues or organs are considered, the more the accuracy of the model is achieved. The dielectric and physiological parameters of 85 kinds of different human tissues or organs were considered in the electromagnetic human body model of this work. The dielectric properties, i.e., permittivity and conductivity, can be found from website of the National Research Council in Italy Institute of Applied Physics, which was prepared by Andreuccetti et al. Some average characteristics of the tissue materials such as skull, brain， and muscle come from the website of FCC. The physiological parameters are thermal conductivity and density. The thermal conductivity values are directly available for almost all the considered tissues from [12]. All these parameters are indexed by image gray value and mapped to the tissues or organs in the electromagnetic model of human body.
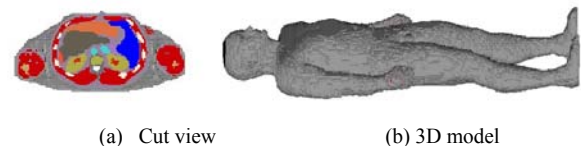

(a) Cut view   (b) 3D model
Fig. 1. Electromagnetic model of human body.

B. Simulation Scenario

The electromagnetic model of human body can be embedded in numerical electromagnetic (EM) simulator which is based on time-domain finite integration technique (FIT) to perform electromagnetic computation. The simulation scenario within the electromagnetic model of human body taken from living males is illustrated in Fig. 2.

The body was exposed to an incoming plane wave from the back. A total of 324 electric and magnetic field probes were placed outside and inside the body from 10 mm to 140 mm depth, with space of 10 mm depth and 20 mm height, respectively. They were located in the middle from left to right side, and embedded in different tissues or organs such as bones, cartilages, blood, and heart, fat, liver, lung and muscles. The incident plane wave was excited with the UWB Gaussian signal for the corresponding frequency bands considered, herein. All of the field probes are ideally frequency independent with a specified polarization, and do not have any coupling among them. Open boundary condition is used for the simulations, and therefore the body environment reflections are considered.
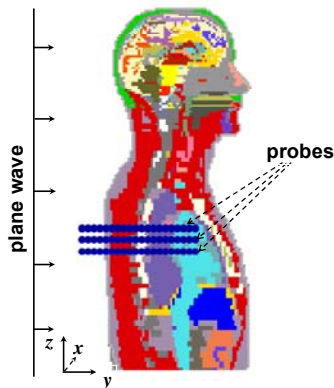

Fig. 2. Simulation scenario of human body with electric and magnetic field probes inside

III. NUMERICAL SIMULATION

Performed EM simulation by utilizing the aforementioned simulation scenario, electric and magnetic field characteristics in the body over 3.0-10.5 GHz band were obtained, and then the average power density and specific absorption rate (SAR) characterization were investigated, and the feasibility and security of wireless communication for implantable devices deep inside the human body were validated.

A. Average Power Density

The US FCC has declared a maximum transmit power density of -41.3 dBm/MHz for UWB. Therefore, even with the full band (i.e. 7.5 GHz) of 3.1-10.6 GHz, the maximum transmitted power is only -2.6 dBm [13], so the signal strength at the receiver becomes important for achieving high data rate transmission, and the strategies to optimize the UWB communication link quality are important too [2]. Average power density is a measurement of signal strength and link quality in the channel. The electromagnetic power density can be computed by the electric and magnetic field. The Poynting vector (**S**) can be used to describe both the power density and the direction of wave propagation, it is depicted as:

$$\mathbf{S} = \mathbf{E} \times \mathbf{H} \qquad (3)$$

where **E** (V/m) and **H** (A/m) are the electrical and magnetic field density, respectively. For incident plane wave propagating along y-axis direction with a horizontal (x-axis) or vertical (z-axis) polarization, the power flux density can be calculated from the Poynting vector along the dominant direction (S_y(t)) into the body. Therefore, the average power density for one observation probe is computed by integrating

the Poynting vector along the dominant direction (S_y(t)) over the observation time [2]. The observation time was chosen to include 99% of the signal power, and it was approximately 200 ns in this work. The average power density for different depths was computed by averaging the power density experienced at each probe on the same plane.

The average power density versus distance from in vitro to back inside is depicted in Fig. 3. It shows that the power density is reduced by distance from the source due to the high loss of the human tissues and organs, and the power loss increases significantly with the increase of transmitted frequency and, with the increase of propagated depth inside body.
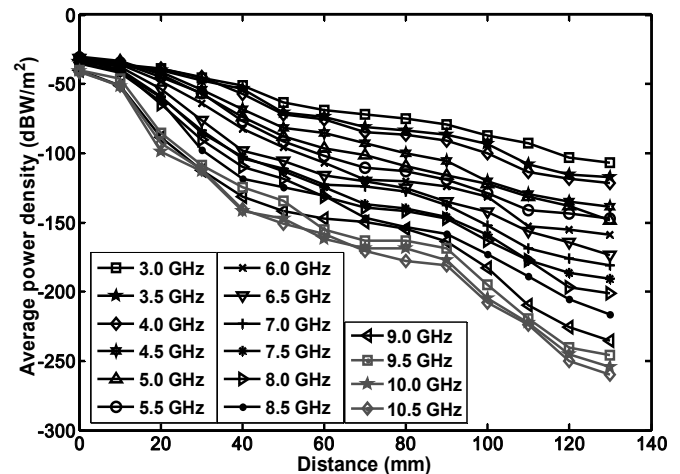

Fig. 3. Average power density inside body versus distance for 3.0-10.5 GHz.

It can be seen from the results in Fig. 3 that the higher frequencies lead to the greater signal attenuation in human body, making their reception almost prohibitive at a deeper distance. However, the UWB communication is still possible for short distances. For instance, when implantable devices are implanted subcutaneously or the implanted depths are less than 3.5cm and they have to communicate with other devices which are either on-body or at short distances outside, the UWB communication is possible. The typical examples are retinal and cochlear in which implant distances are a few centimeters. Assuming an UWB transceiver with a band width of 500 MHz and a maximum transmitted power density limit of -41.3dBm/MHz is adopted, the maximum transmit power is -14.3 dBm. It can still bear a path loss of 80 dB and make UWB wireless communication possible for a typical receiver whose sensitivity is -95 dBm. On the other hand, since the human body is a high lossy medium and the transmitter for an implantable device is always embedded inside the body, it should be able to transmit more than -41.3 dBm/MHz while it still accommodates the FCC requirement outside the body [14]. For instance, based on Fig. 3, the transmit power level can be arranged for a typical receiver with a sensitivity of -95 dBm, as illustrated in Fig. 4. The deeper the penetration depth is (i.e., the deeper the transmitter is implanted into the human body), the higher the transmission power are required.

B. Specific Absorption Rate (SAR)

Recently, the most recognized radio-frequency (RF) protection standards adopt the SAR as the basic parameter to establish the safety of human body exposure in the high
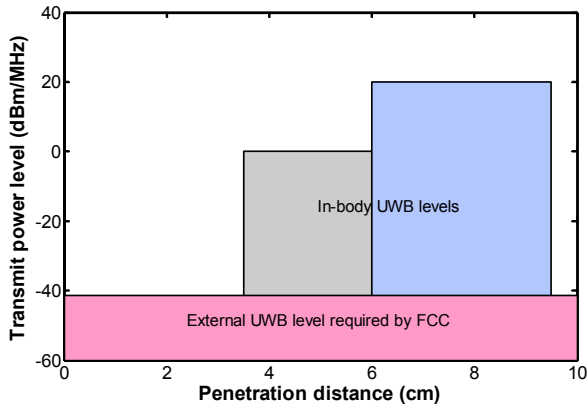
frequency bands.

Fig. 4. Power level arrangement for transmitted UWB signal in body

Specific absorption rate (SAR) is the unit of measurement for the amount of radio-frequency energy absorbed by tissues or organs when exposed to electromagnetic field. It is defined as the time derivative of the incremental energy (dW) absorbed by (dissipated in) an incremental mass (dm) contained in a volume element (dV) of a given density (ρ):

$$SAR = \frac{d}{dt}\left(\frac{dW}{dm}\right) = \frac{d}{dt}\left(\frac{dW}{\rho dV}\right) . \quad (4)$$

Another mathematical expression which relates SAR to the electric field is shown below:

$$SAR = \frac{p}{\rho} = \frac{\sigma E^2}{2\rho} = \frac{J^2}{2\rho\sigma} , \quad (5)$$

where p is power loss density, J is current density, σ is conductivity, and E is electric field amplitude in tissue. Values of *SAR* depend on the incident field parameters and the characteristics of the exposed body, i.e., its size and external and internal geometry, and the dielectric properties of the various tissues.

The human body model allows the evaluation of local SAR as averaged over 1 g and 10 g all along the body. The SARs in different frequencies were evidenced by performed EM simulations. The max SAR, average SAR over 1 g and average SAR over 10 g absorbed by human body in 3.0-10.5 GHz band are listed on Table I.

As the guidelines from the International Commission on Non-Ionizing Radiation Protection (ICNIRP) [15]: the

localized SARs of head and trunk for human body in 10 MHz-10 GHz frequency band are under 2 W/kg. It can be seen from Table I that the SAR values absorbed by human body in 3.0-10.5 GHz band are under the limit of ICNIRP, so using this band for implantable devices' wireless communication is secure.

IV. CHANNEL MODELING

The path gain is a measure for the average attenuation of the signal from transmitter to receiver. It obviously depends on the distance between receiver and transmitter and, together with the transmit power, determines the range of a wireless system: for distances beyond a certain range, the received signal becomes so week that proper reception is not possible anymore [16]. The path gain modeling is needed to estimate the signal energy at different distances from the source. The distance dependent path gain for both indoor and free space were modeled with the classical power law (the logarithmic function) [16] given as

$$G_p(d) = G_{p0} + 10n \log_{10}\left(\frac{d}{d_0}\right), \quad (6)$$

where, G_{p0} is a power scaling constant, d is the distance between the end and source, and n corresponds to the path gain factor (propagation exponent). The path gain factor depends on the environment in which the system operates, for free space propagation, n=-2 is valid, the typical values for line-of-sight (LOS) are on the order of -1.5, and for non-LOS on the order of -3 to -4. Due to the influence of lossy tissues and organs, the path gain for both outside and inside the human body calculated from (6) does not fit with the simulated data in Fig. 3. Hence, the classical power law is modified as

$$G_p(d) = G_{p0} + 10n \log_{10}\left(\frac{(d + d_0)}{d_0}\right). \quad (7)$$

The EM simulation results and numerical computation results from (7) are depicted in Fig. 5. It can be seen that the proposed numerical model produces a good approximation. The minimum and average root-mean-square error (RMSE) is 4.3 and 9.8, respectively. All of these fitted path gain factor (n), power scaling constant (G_{p0}) and d_0 for band of 3.0-10.5 GHz are tabulated in Table II. It can be seen that the path gain factors (n) in human body are -6.5 to -11.0 for 3.0-10.5 GHz band, which indicates that the higher frequency is transmitted,

TABLE I
SUMMARY OF SAR BY HUMAN BODY IN 3.0-10.5 GHz BAND

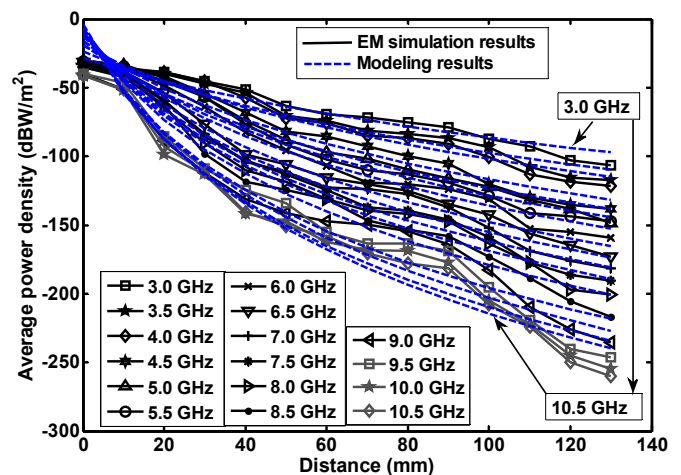| Frequency (GHz)	Max. SAR (W/kg)	10g SAR (mW/kg)	1g SAR (mW/kg)
3.00	0.013	0.073	0.15
3.50	0.012	0.068	0.16
4.00	0.009	0.064	0.18
4.50	0.012	0.071	0.17
5.00	0.010	0.077	0.19
5.50	0.009	0.084	0.24
6.00	0.010	0.091	0.26
6.50	0.012	0.088	0.27
7.00	0.015	0.088	0.26
7.50	0.015	0.089	0.26
8.00	0.015	0.088	0.27
8.50	0.009	0.095	0.26
9.00	0.100	0.101	0.29
9.50	0.007	0.098	0.29
10.0	0.010	0.110	0.30
10.5	0.009	0.100	0.25

Fig. 5. EM simulation results and modeling results of average power density inside body versus distance

TABLE II
FITTED PATH GAIN FACTOR (*n*), POWER SCALING CONSTANT (G_{P0}) AND d_0
FOR 3.0-10.5 GHZ

Frequency (GHz)	n	G_{p0}	d_0
3.00	-6.5	-28.7	70
3.50	-6.7	-23.7	50
4.00	-7.0	-19.7	45
4.50	-7.3	-16.7	34
5.00	-7.5	-18.7	33
5.50	-7.7	-15.7	30
6.00	-7.8	-12.7	26
6.50	-8.0	-10.7	22
7.00	-8.2	-12.7	21
7.50	-8.5	-9.70	20
8.00	-9.1	-9.70	21
8.50	-9.6	-7.00	20
9.00	-10.0	-7.70	18
9.50	-10.7	-6.60	19
10.0	-10.8	-6.70	18
10.5	-11.0	-6.70	18

the severer power loss is undergone.

V. CONCLUSIONS

By performing electromagnetic (EM) simulation based on an electromagnetic human model, it is found that the max SAR, average SAR over 1 g and over 10 g absorbed by human body in 3.0-10.5 GHz band are in accordance with the criterions of ICNIRP, substantiating the security of using this band for wireless communication of implantable devices.

The loss of average power density at the different depths of human body indicates the feasibility of using 3.0-10.5 GHz UWB band for the wireless communication of implantable devices. For devices with implanted depth less than 3.5 cm, the full band 3.0-10.5 GHz of UWB can be applied to wireless communication while it still accommodates the requirement of FCC. For further deep implantable devices, the lower sub-band of UWB should be applied to wireless communication to accommodate the requirement of FCC, or the devices in the body should transmit more than -41.3 dBm/MHz to guarantee the proper communication and make the signal level accommodate FCC's requirement outside the body. Finally, the transmit power level for typical receiver has been arranged.

A modified classical power law function can be adopted to depict the in vivo distance-depended path gain. The channel numerical statistical model describing the in-body propagation channel characterizations has a simple form, making it unnecessary for the designers of implantable devices to use a complexity EM simulation which causes extremely long computational time.

REFERENCES

[1] O. Novak, C. Charles, and B. R. Brown, "An area and power efficient I-UWB transmitter for biomedical applications implemented in 65 nm CMOS technology," in *Proc. IEEE Conf. on Biomedical Circuits and Systems,* San Diego, 2011, pp. 177-180.

[2] A. Khaleghi, I. Balasingham, and R. Chávez-santiago, "Computational study of ultra-wideband wave propagation into the human chest," *IET Microwaves Antennas Propagation,* vol. 5, no. 5, pp. 559-567, May 2011.

[3] E. G. Lim, J. C. Wang, Z. Wang, T. Tillo, and K. L. Man, "The UHF band in-body antennas for wireless capsule endoscopy," *Engineering Letters*, vol. 21, no. 2, pp. 72-80, May 2013.

[4] M. S. Chae, Z. Yang, M. R. Yuce, L. Hoang, and W. Liu, "A 128-channel 6 mW wireless neural recording IC with spike feature extraction and UWB transmitter," *IEEE Transaction on Neural System and Rehabilitation Engineering*, vol. 17, no. 4, pp. 312-321, Aug. 2009.

[5] A. Khaleghi, R. Chávez-santiago, and I. Balasingham, "Ultra-wideband pulse-based data communications for medical implants," *IET Communications*,Vol. 4, no. 15, pp. 1889-1897, Oct. 2010.

[6] Q. Wang, K. Massami, and J. Q. Wang, "Channel modeling and BER performance for wearable and implant UWB body area links on chest," in *Proc. IEEE International Conf. on Ultra-Wideband*, New Jersey, 2009, pp. 316-320.

[7] H. Bahrami, B. Gosselin, and L. A. Rusch, "Realistic modeling of the biological channel for the design of implantable wireless UWB communication systems," in *Proc. 34th Annual International Conference of the IEEE Engineering in Medicine and Biology Society,* San Diego, 2012, pp. 6015-6018.

[8] B-L Wei, H-W Yue, Q. Zhou, W-L Xu, X-M Wei, and J-H Duan, "Modeling of in-body propagation characterization for 2.5/3.5 GHz implantable devices applications," *Applied Mechanics and Materials,* Vol. 273, pp. 583-587, Jan. 2013.

[9] S. Gabriely, R. W. Lau, and C. Gabriel, "The dielectric properties of biological tissues: III, parametric models for the dielectric spectrum of tissues," *Physics in Medicine and Biology,* vol. 41, no. 11, pp. 2271–2293, Nov. 1996.

[10] I. G. Zubal, C. R. Harrell, E. O. Smirh, Z. Rattner, G. Gindi, and P. B. Hoffer, "Computerized three-dimensional segmented human anatomy," *Medical Physics*, vol. 21, no. 2, pp. 299-302, Feb. 1994.

[11] M. J. Ackerman, "Viewpoint: The visible human project," *Journal Biocommuncation*. Vol. 18, no. 2, pp. 14-19, Aug. 1991.

[12] K. R. Holmes, "Thermal conductivity data for specific tissues and organs for humans and other mammalian species," [Online]. Available: http://users.ece.utexas.edu/~valvano/research/Thermal.pdf

[13] L. Zhao, S-P Liu, L. Jin, and J-Y Chen, "Research on the power spectral density limit in UWB systems," *Telecommunications Science,* vol. 27, no. 2, pp. 34-39, Feb. 2011.

[14] M. R. Yuce, H. C. Keong, and M. S. Chae, "Wideband communication for implantable and wearable systems," *IEEE Transactions on Microwave Theory and Techniques,* vol. 57, no. 10, pp. 2597-2604, Oct. 2009.

[15] International Commission on Non-ionizing Radiation Protection, "For limiting exposure to time-varying electric, magnetic and electromagnetic fields (up to 300GHz)," *Health Physics*, vol. 74, no. 4, pp. 494-522, Apr. 1998.

[16] A. F. Molisch, "Ultra-wide-band propagation channels," *Proceeding of the IEEE*. vol. 97, no. 2, pp. 353-371, Feb. 2009.